

AD-A123 057

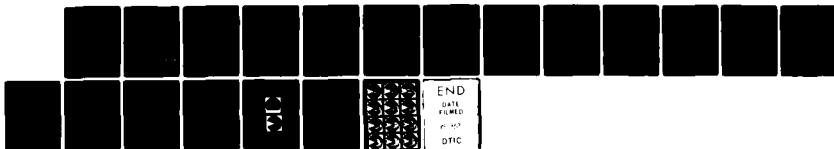
A WAXICON MIRROR-ELECTRODE FOR LASER INITIATED  
DISCHARGE CHANNELS(U) MICHIGAN UNIV ANN ARBOR LASER  
PLASMA RESEARCH LAB R M GILGENBACH 30 SEP 82  
LPRL-TR-111 N00014-81-K-0700

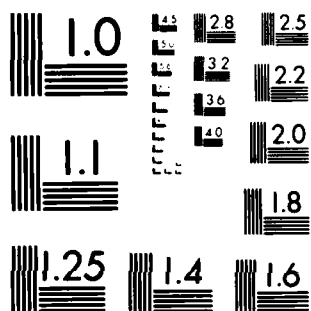
1/1

UNCLASSIFIED

F/G 20/5

NL





MICROCOPY RESOLUTION TEST CHART  
NATIONAL BUREAU OF STANDARDS 1963-A

LPRL\*

12

AD A123057

A Waxicon Mirror-Electrode for  
Laser Initiated Discharge Channels

R. M. Gilgenbach

Technical Report #111  
September 30, 1982



Technical Report  
Department of Nuclear Engineering  
Laser Plasma Research Laboratory

DISTRIBUTION STATEMENT A

Approved for public release;  
Distribution Unlimited

DTIC  
ELECTE  
S JAN 6 1983 D

82 12 22 075

REPORT DOCUMENTATION PAGE		READ INSTRUCTIONS BEFORE COMPLETING FORM
1. REPORT NUMBER Technical Report #111	2. GOVT ACCESSION NO. <b>AD-A223057</b>	3. RECIPIENT'S CATALOG NUMBER
4. TITLE (and Subtitle) A Waxicon Mirror - Electrode for Laser Initiated Discharge Channels	5. TYPE OF REPORT & PERIOD COVERED Interim Report	
7. AUTHOR(s) R.M. Gilgenbach	6. PERFORMING ORG. REPORT NUMBER #111	
9. PERFORMING ORGANIZATION NAME AND ADDRESS The University of Michigan Ann Arbor, MI 48109	8. CONTRACT OR GRANT NUMBER(s) N00014-81-K-0700 NR-012-756	
11. CONTROLLING OFFICE NAME AND ADDRESS Office of Naval Research Arlington, VA 22217	10. PROGRAM ELEMENT, PROJECT, TASK AREA & WORK UNIT NUMBERS	
14. MONITORING AGENCY NAME & ADDRESS (if different from Controlling Office)	12. REPORT DATE Sept. 30, 1982	
	13. NUMBER OF PAGES 16	
	15. SECURITY CLASS. (of this report) Unclassified	
	15a. DECLASSIFICATION/DOWNGRADING SCHEDULE	
16. DISTRIBUTION STATEMENT (of this Report) Approved for public release; distribution unlimited		
17. DISTRIBUTION STATEMENT (of the abstract entered in Block 20, if different from Report)		
18. SUPPLEMENTARY NOTES		
19. KEY WORDS (Continue on reverse side if necessary and identify by block number) Channel Focusing System Waxicon		
20. ABSTRACT (Continue on reverse side if necessary and identify by block number) A reflecting waxicon (compound axicon) has been demonstrated to generate a smooth CO <sub>2</sub> laser-induced breakdown plasma in atmospheric pressure air. The protruding central cone of the waxicon also functions as an electrode for 30 kV laser initiated discharges. The waxicon mirror-electrode has several advantages over conventional focusing systems for laser initiated discharges in unfiltered air: (continued on back)		

## ABSTRACT(continued)

- (1) Smoother laser induced breakdown plasma,
- (2) Concentration of laser energy deposition in the plasma near the tip of the electrode,
- (3) More compact laser initiated discharge experiments since long focal length lenses or mirrors are not required, and
- (4) A self contained focusing system - electrode for laser triggered switches.

At times later than 250 $\mu$ s after discharge initiation, shock waves reflected from the waxicon have been shown to propagate longitudinally along the discharge axis. The scaling of the waxicon-focused breakdown plasma length has been measured as a function of incident laser energy.

Accession For	
NTIS GRA&I	<input checked="" type="checkbox"/>
DTIC TAB	<input type="checkbox"/>
Unannounced	<input type="checkbox"/>
Justification	
By _____	
Distribution/	
Availability Codes	
Avail and/or	
Dist	Special
A	

A Waxicon Mirror-Electrode for  
Laser Initiated Discharge Channels

R.M. Gilgenbach  
Department of Nuclear Engineering  
The University of Michigan  
Ann Arbor, MI 48109

Abstract

A reflecting waxicon (compound axicon) has been demonstrated to generate a smooth CO<sub>2</sub> laser-induced breakdown plasma in atmospheric pressure air. The protruding central cone of the waxicon also functions as an electrode for 30 kV laser initiated discharges. The waxicon mirror-electrode has several advantages over conventional focusing systems for laser initiated discharges in unfiltered air:

- 1) Smoother laser induced breakdown plasma,
- 2) Concentration of laser energy deposition in the plasma near the tip of the electrode,
- 3) More compact laser initiated discharge experiments since long focal length lenses or mirrors are not required, and
- 4) A self contained focusing system - electrode for laser triggered switches.

At times later than 250 $\mu$ s after discharge initiation, shock waves reflected from the waxicon have been shown to propagate longitudinally along the discharge axis. The scaling of the waxicon-focused breakdown plasma length has been measured as a function of incident laser energy.

## I. Introduction

Laser initiated discharges<sup>1-4</sup> have a number of applications concerning laser triggered switches, artificial lightning, as well as recent interest as a means of transporting particle beams through gas blankets in inertial confinement fusion reactors<sup>5-7</sup>. Experiments on laser initiated discharges reported to date have employed long focal length lenses or mirrors to generate a chain of breakdown beads which are randomly distributed for each pulse<sup>1-4</sup>. A smooth, uniform, laser induced breakdown plasma could provide more reproducible laser initiated breakdown for switches and could possibly improve the reproducibility of reduced density channels generated from such discharges. One problem with using conventional focusing systems for laser initiated discharges is that the discharge electrode placement can vary from day to day, depending upon dust and atmospheric conditions which affect the position of the laser induced breakdown beads. The waxicon-electrode has been demonstrated here to produce a smooth, narrow, straight, laser-induced breakdown plasma which begins at the tip of the high voltage electrode.

## II. Waxicon Design and Experimental Configuration

This article describes the design and experimental performance of a modified waxicon (double reflecting axicon with a W-shaped cross section). The inner cone of the waxicon also functions as the electrode for laser guided discharges. A cross sectional view of the device is depicted in Fig. 1a. Waxicons which have been used in the past to convert annular laser beams to collimated, solid beams have generally been of a symmetric design with:

$$\phi_1 = \phi_2 = 45^\circ \quad , \quad (\text{Eq. 1})$$

where the angles are defined in Fig. 1a.

However, by increasing the total angle,  $\phi_w$  , to a value greater than  $90^\circ$ , the beam can be made to overlap into a quasi line-focus as depicted in Fig. 1b. The angle (  $\theta$  ) at which a ray crosses the axis is given by:

$$\theta = 2\phi_w - 180^\circ \quad (\text{Eq. 2})$$

Thus, for the typical waxicon design, (  $\phi_w = 90^\circ$  ) the exiting beam is collimated. For generating laser induced breakdown at the peak power levels (  $\leq 0.3\text{GW}$  ) of our  $\text{CO}_2$  laser, it was necessary to increase  $\phi_w$  to  $93.5^\circ$ , since the resulting beam overlap (Fig. 1b) raises the power density above the clean air breakdown threshold. Note that because the  $\text{CO}_2$  laser beam has an elongated annular shape, (Fig. 2), it was necessary to employ a circular, inner beam aperture to prevent power from impinging at the intersection of the inner and outer waxicon cones. This reduced the incident power to 90.3% of the laser power.

The angles  $\phi_1$  , and  $\phi_2$  were chosen so that the outermost part of the elongated beam (ray 1 in Fig. 1b) would cross directly in front of the inner waxicon cone in order to deposit this laser energy near the electrode tip. Most of the  $\text{CO}_2$  laser power in our experiment was concentrated near rays 1 and 2 in Fig. 1b. The central beam dump diameter (5.2cm) was chosen to be slightly larger than the inner cone diameter (5cm). Thus, there should be negligible power in ray 3, which corresponds to the diameter of the beam dump.

Another design constraint upon this device concerned the use of the waxicon as an electrode. This required that the central cone protrude from the waxicon to prevent the discharge from arcing to the outer edges of the waxicon. To satisfy this condition  $\phi_1$  must be greater than  $\phi_2$  . The resultant design shown in Fig. 1a meets the requirements for both the focusing system and the electrode.

The waxicon-electrode was fabricated from a solid bar of brass on a standard lathe. Polishing was performed on the lathe with a succession of fine sandpaper (400 and 600 grit), followed by optical polishing compounds (#500 and #1000). The resultant surface had a finish which was sufficient to perform alignment with a helium neon laser beam expanded through the unstable resonator of the  $\text{CO}_2$  laser. Scratches from the machining operation were still visible on the finished waxicon, which may account for what appears to be some surface arcing at the highest power levels (presented in the data of Section III). Since the surface resistivity of brass is more than twice that of gold,

the power loss of the waxicon will be correspondingly increased over that of the gold mirror typically employed in these experiments.

Configuration of the waxicon-electrode in the laser guided discharge experiment is illustrated in Fig. 2. The waxicon was electrically isolated from its supports and connected to the discharge circuitry by 5 cm wide, low inductance braided cable. Incident  $\text{CO}_2$  laser energy (in a 100ns triangular pulse) was controlled by means of a propylene absorption cell. The spark gap switch was triggered  $5\mu\text{s}$  after the  $\text{CO}_2$  laser pulse in these experiments. For the 30 kV capacitor voltage the discharge current was 12 kA with a  $2.5\mu\text{s}$  ringing period and  $1/e$  decay time of  $11\mu\text{s}$ . The laser induced plasma and discharge channel dynamics were characterized by a ruby laser Schlieren diagnostic<sup>4,8</sup> which utilized a pinhole to obtain 2 dimensional spatial resolution. Adjustment of the ruby laser pulse timing on separate discharges permitted a study of the temporal evolution of the channel.

### III. Experimental Results

Laser induced air breakdown from the waxicon focus is compared with that of a 2.5m focal length gold mirror in Fig.

3. The waxicon focus apparently generates a much smoother breakdown plasma than the conventional long focal length mirror. Although for this design the waxicon air breakdown length is shorter, there are no major gaps or striations in the waxicon-generated plasma as there are with the standard focus. This effect can be explained theoretically<sup>8</sup> by noting that in the case of the long focal length mirror the laser induced breakdown occurs from natural atmospheric aerosols, whereas the waxicon increases the optical intensity above the clean air breakdown threshold over a smooth, straight, narrow region beginning at the electrode.

Our previous experiments<sup>9</sup> have also demonstrated that this effect cannot be duplicated in unfiltered air by a conventional short focal length lens because although the clean air breakdown threshold can be exceeded, the laser induced breakdown spark is large and characteristically pear shaped rather than the straight, narrow, waxicon-electrode plasma.

The production of plasma off the surface of the center cone is in fact a desirable design feature, since it ensures that the laser induced breakdown extends outward from the tip of the electrode. (That the waxicon plasma is slightly below the center of the cone can be attributed to a slight misalignment).

The length of laser induced plasma from the waxicon was measured as a function of incident laser energy, with the results plotted in Fig. 4. At the incident energy levels just above breakdown, the laser induced plasma length increases more rapidly than at the higher energies. This decrease in the slope of Fig. 4 can be explained in terms of the variation of the laser intensity along the axis (Fig 1b). The schlieren photographs indicated that as the incident laser energy was increased, the density gradients in the air breakdown plasma increased. This implies that more of the incident laser energy was being absorbed in the relatively short plasma channel near the electrode tip.

The stability of the hot gas dynamics in the vicinity of the electrodes was tested by taking a sequence of schlieren photographs at a number of different times following discharge initiation. The results, presented in Fig. 5, clearly illustrate the shock wave and the expanding reduced density region in the early stages of gas dynamic evolution (0.7 $\mu$ s to 51  $\mu$ s). At times greater than 100 $\mu$ s after discharge initiation, the hot gas appears to be more turbulent near the right hand electrode than near the waxicon. There are no significant changes in the gas dynamics between 100 $\mu$ s and 200 $\mu$ s, however, at 200 $\mu$ s a shock wave reflected from the waxicon is visible near the left hand side of the photo. Between 250 $\mu$ s and 350 $\mu$ s this shock wave can be seen to propagate longitudinally along the axis, possibly accounting for some increase in the level of turbulence. Previous experiments<sup>10</sup> have demonstrated that

shock waves which propagate transversely to hot gas channels decrease the channel stability and drive fine scale turbulence. In the data of Fig. 5, the longitudinally propagating shock wave does not appear to have as great an influence on turbulent behavior. Since channel turbulence results from convective mixing of hot channel air with cool outside air<sup>4</sup>, the different effects of longitudinal and transverse shocks could be due to the larger mass of cool air transported into the hot gas region by transverse shocks, which act along the entire channel length<sup>10</sup>.

Slight erosion of the inner waxicon cone-electrode was noted after some 30 discharges. In the case of our brass prototype, the damaged surface can easily be repolished. An improved waxicon-electrode design consists of a two piece waxicon, where the inner cone is removable for polishing or replacement.

In conclusion, the generation of reproducible laser induced breakdown plasmas which extend outward from the tip of the electrode makes this a promising configuration for a laser triggered switch.

Acknowledgements

Technical support from L. Smutek and experimental assistance from L.D. Horton and O.E. Ulrich are gratefully acknowledged. Dr. J.R. Greig provided valuable suggestions and encouragement regarding the waxicon design and construction. This research was supported by the Office of Naval Research, Project NR-012-756.

### References

- 1) J.R. Greig, D.W. Koopman, R.F. Fernsler, R.E. Pechacek, I.M. Vitkovitsky, and A. W. Ali, Phys. Rev. Lett. 41 174 (1978)
- 2) J.R. Greig, Bull. Am. Phys. Soc., 25 942 (1980)
- 3) D.W. Koopman and K.A. Saum, J. Appl. Phys.. 44 5328 (1973)
- 4) J.M. Picone, J.P. Boris, J.R. Greig, M. Raleigh, and R.F. Fernsler, J. Atmos, Science 38 2056 (1981).
- 5) G. Yonas, Sci. Amer., 239 50 (1978)
- 6) P.A. Miller, R.I. Butler, M. Cowan, J.R. Freeman, J.W. Poukey, T.P. Wright, and G. Yonas, Phys. Rev. Lett. 39 92 (1977)
- 7) J.R. Freeman, L. Baker, and P.C. Cook, Nuc. Fusion, 22 383 (1982)
- 8) J.R. Greig (Private Communication)
- 9) R.M. Gilgenbach, O.E. Ulrich, L.D. Horton, and J. Meachum, Bull. Am. Phys. Soc. 27 1028 (1982)
- 10) L.D. Horton and R.M. Gilgenbach, Phys. Fluids, 25 1702 (1982)

Figure Captions

Fig. 1. a) Cutaway view of waxicon design,  
b) Ray diagram illustrating region of overlap  
for CO<sub>2</sub> laser beam.

Fig. 2. Experimental configuration illustrating waxicon -  
electrode placement.

Fig. 3. Ruby laser schlieren photographs of laser induced  
breakdown plasma for:

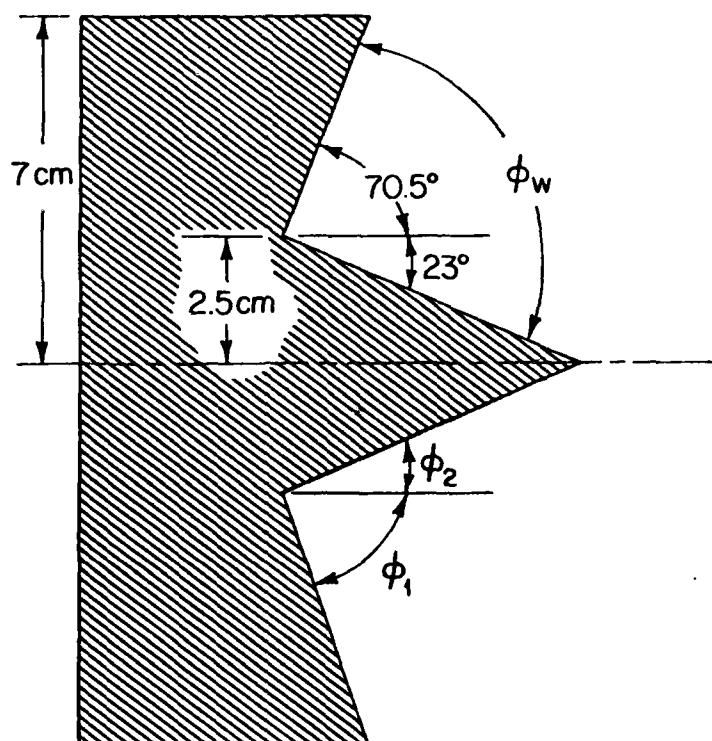
- a) 2.5 m focal length gold mirror located to left  
of photograph,
- b) Waxicon mirror-electrode; the inner cone is  
visible as a shadow on the left hand side of  
the photograph.

The circular schlieren field of view has a diameter  
of 8 cm.

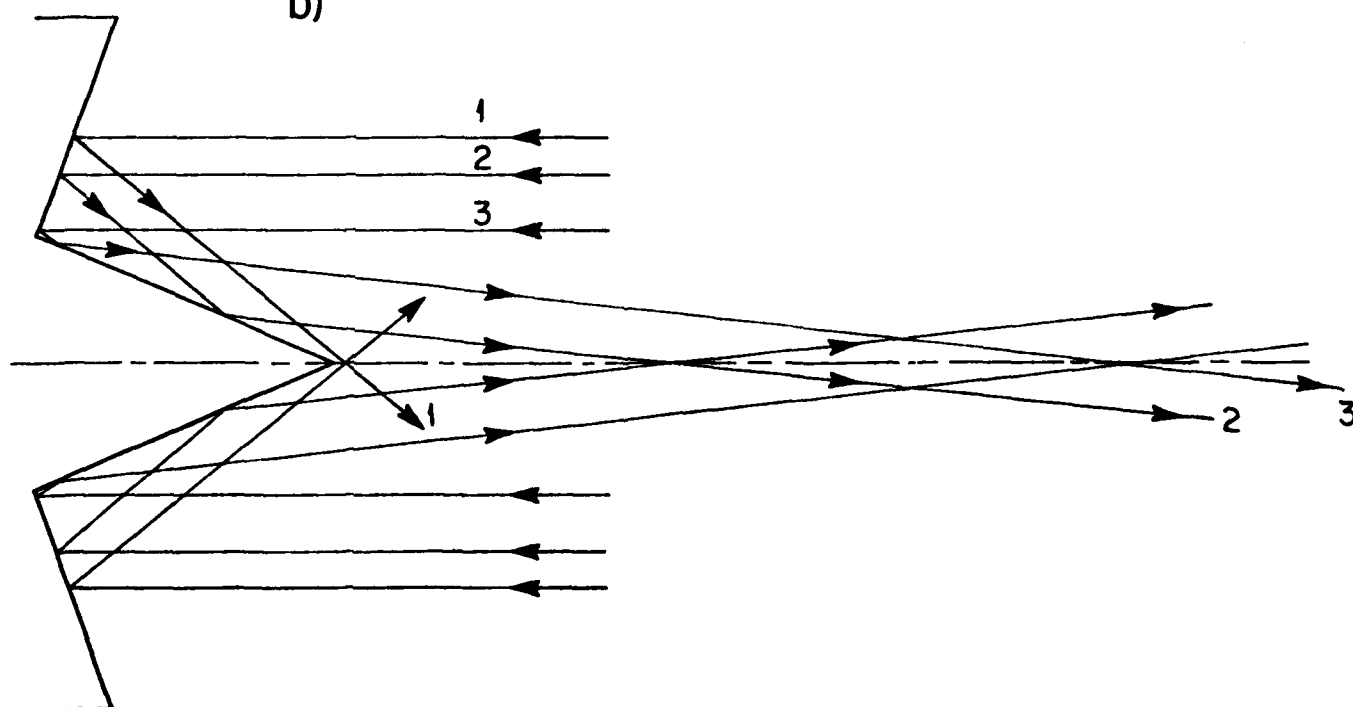
Fig. 4. Length of laser-induced breakdown plasma from the  
waxicon focus as a function of incident laser energy  
in a 100 ns pulse. Data obtained from schlieren  
photographs taken 0.5 $\mu$ s after laser pulse.

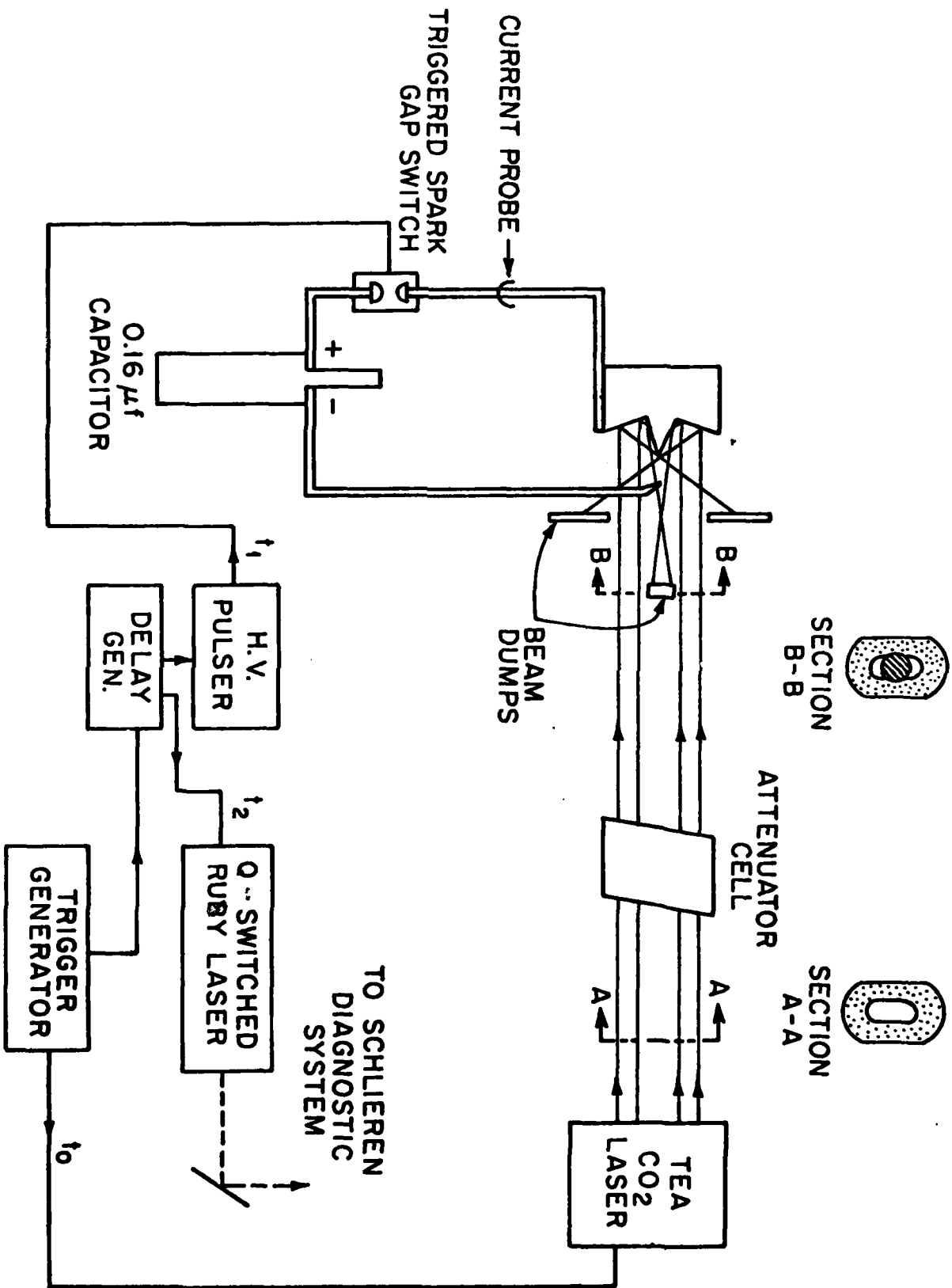
Fig. 5. Sequence of schlieren photographs for waxicon -  
focused laser-initiated discharge channels. Times  
listed at the upper corner of each photograph  
represent the delay between discharge initiation  
and the schlieren ruby laser pulse.

a)



b)

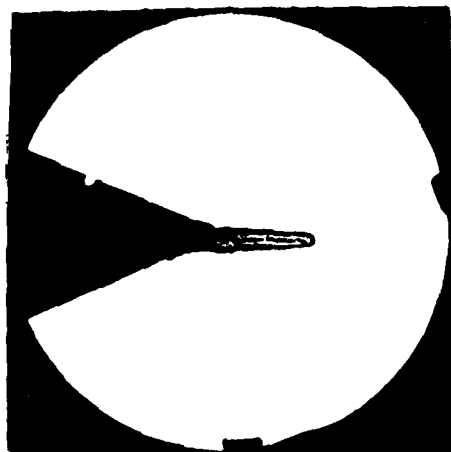


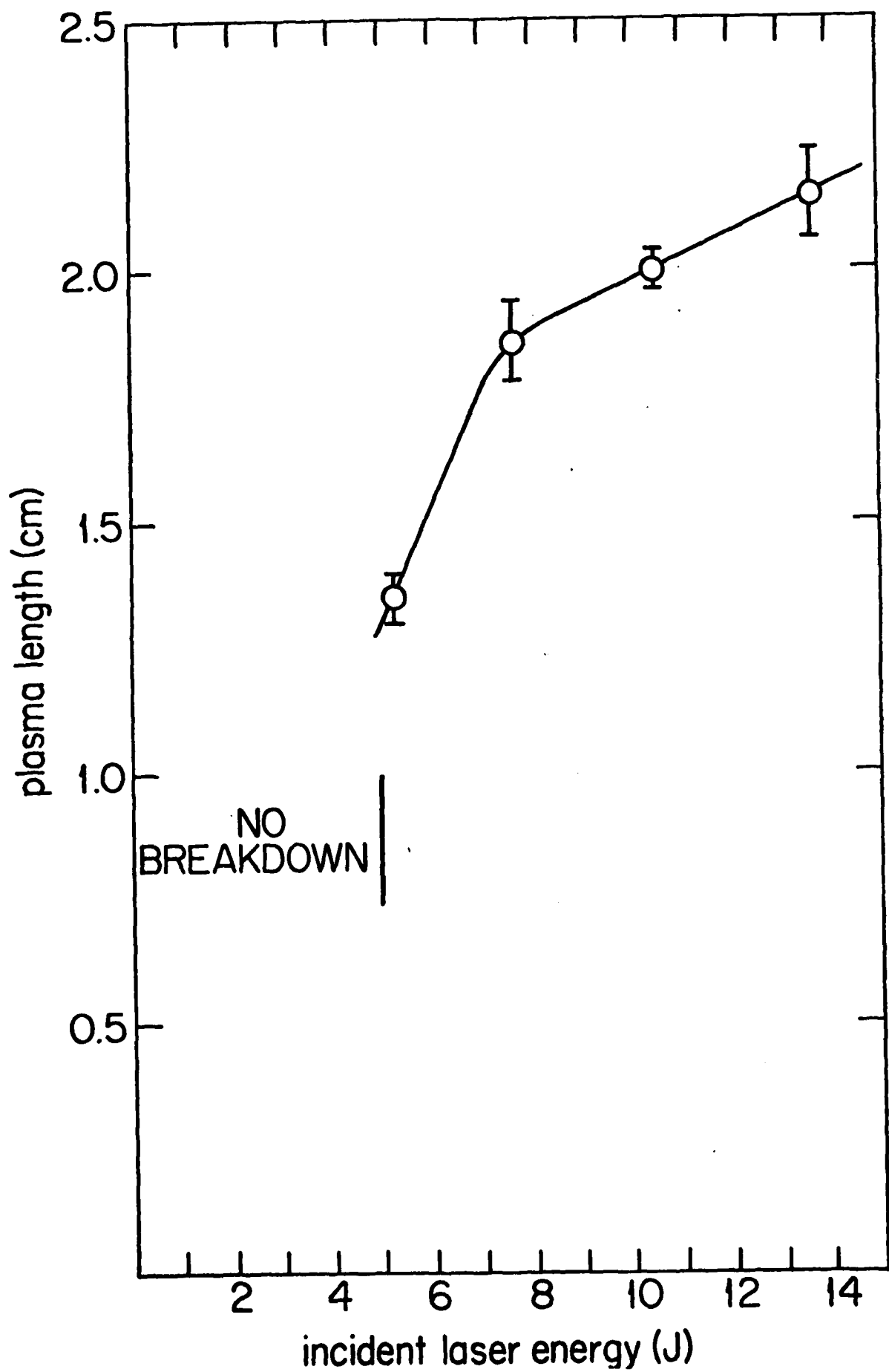


a)

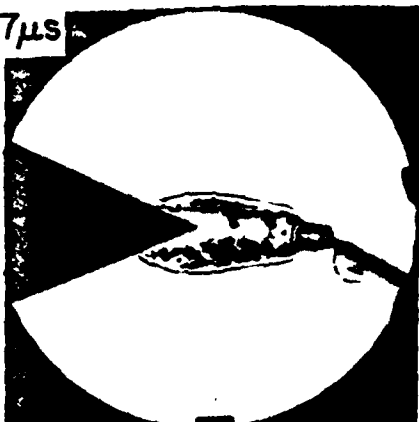


b)

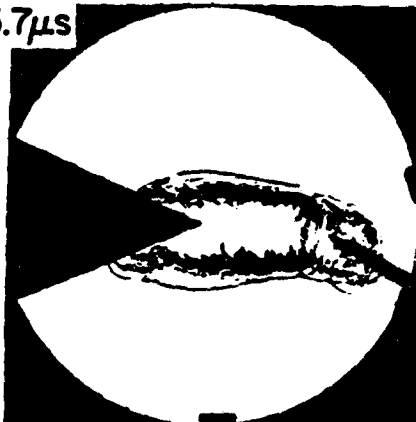




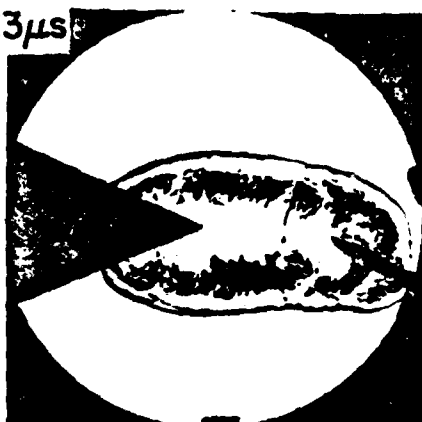
0.7 $\mu$ s



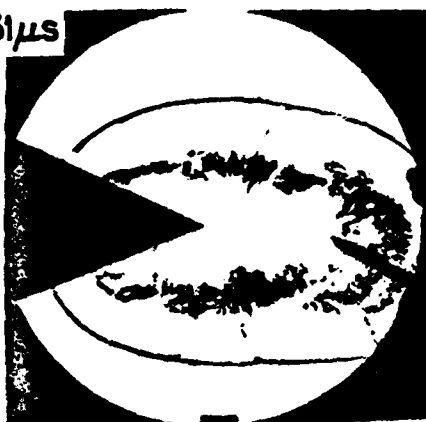
5.7 $\mu$ s



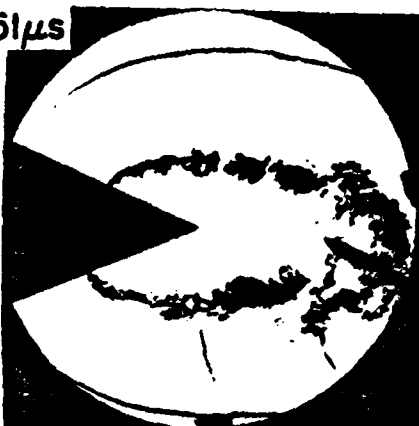
13 $\mu$ s



31 $\mu$ s



51 $\mu$ s



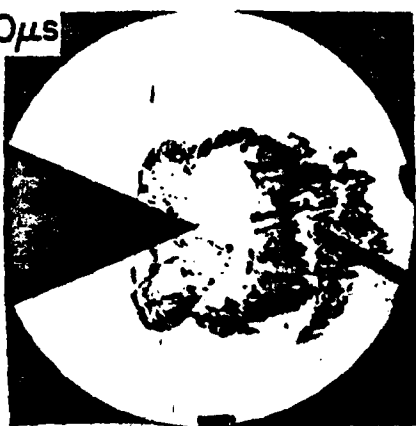
100 $\mu$ s



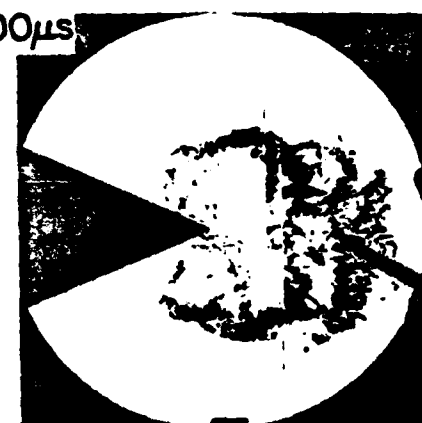
200 $\mu$ s



250 $\mu$ s



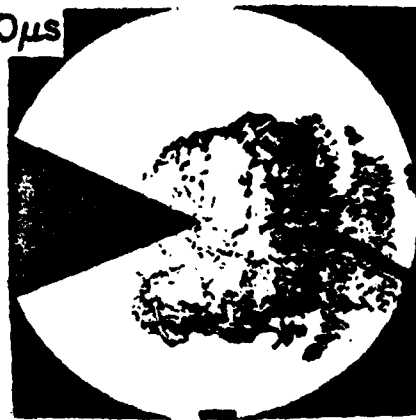
300 $\mu$ s



350 $\mu$ s



400 $\mu$ s



500 $\mu$ s

